CrossMark

Investigating membrane fouling associated with GAC fluidization on membrane with effluent from anaerobic fluidized bed bioreactor in domestic wastewater treatment

Muhammad Aslam[1] · Jeonghwan Kim[1]

Abstract Effect of mechanical scouring driven by granular activated carbon (GAC) fluidization on membrane fouling was investigated using a laboratory-scaled, fluidized membrane reactor filtering the effluent from anaerobic fluidized bed bioreactor (AFBR) in domestic wastewater treatment. The GAC particles were fluidized by recirculating a bulk solution only through the membrane reactor to control membrane fouling. The membrane fouling was compared with two different feed solutions, effluent taken from a pilot-scaled, AFBR treating domestic wastewater and its filtrate through 0.1-μm membrane pore size. The GAC fluidization driven by bulk recirculation through the membrane reactor was very effective to reduce membrane fouling. Membrane scouring under GAC fluidization decreased reversible fouling resistance effectively. Fouling mitigation was more pronounced with bigger GAC particles than smaller ones as fluidized media. Regardless of the fluidized GAC sizes, however, there was limited effect on controlling irreversible fouling caused by colloidal materials which is smaller than 0.1 μm. In addition, the deposit of GAC particles that ranged from 180 to 500 μm in size on membrane surface was very significant and accelerated fouling rate. Biopolymers rejected by the membranes were thought to play a role as binding these small GAC particles on membrane surface strongly.

✉ Jeonghwan Kim
jeonghwankim@inha.ac.kr

[1] Department of Environmental Engineering, Inha University, 100 Inha-ro, Namgu, Incheon, Republic of Korea

Introduction

Anaerobic membrane bioreactor (AnMBR) is a MBR technology being found immense potential for various industrial wastewater treatment applications due to its distinct advantages over conventional aerobic MBR technologies (Liao et al. 2006; Lin et al. 2012). The AnMBRs have been tested specifically with synthetic, food processing, chemical, pulp and paper, textile, pharmaceutical, petroleum, and wastewaters with high solid contents at laboratory-, pilot-, and full-scaled operation of them (Liao et al. 2006; Lin et al. 2012). Recently, the applications of AnMBRs have been extended for domestic wastewater treatment, mainly owing to energy recovery in the form of methane and less production of biosolids (Ghauri et al. 2011; Ozgun et al. 2013; Smith et al. 2012). With the AnMBR treating domestic wastewater, membrane can retain biomass completely, producing high effluent (permeate) quality at long solid retention time (SRT) under relatively short hydraulic retention time (HRT) (Charfi et al. 2012; Meng et al. 2017; Skouteris et al. 2012; Stuckey 2012). However, membrane fouling caused by deposition of foulant materials present in the wastewater on membrane surface and/ or within membrane pore matrix should be still main hurdle to be resolved (Ahmad et al. 2016; Aslam et al. 2015; Díaz et al. 2016; Hu et al., 2012; Yu et al. 2017).

Biogas sparging along membrane surface has been widely applied to reduce membrane fouling within the AnMBR system (Aslan et al. 2014). However, biogas sparging to reduce concentration polarization layer or cake layer from the membrane requires much energy consumption ranging from 0.7 to 3.4 kWh/m^3 (Aslam et al. 2017a; Le-Clech et al. 2006; Meng et al. 2009; Wang et al. 2014), which is even higher than the energy required by aerobic MBR system (0.5–1.0 kWh/m^3) (Krzeminski et al. 2012; Martin et al. 2011). Recently, gas sparging is often combined with suspended carriers to reduce energy cost in fouling control (Alresheedi and Basu 2014; Ng et al. 2013; Huang et al. 2008; Jin et al. 2013; Nguyen et al. 2016; Pradhan et al. 2012). Movement of suspended carriers under the biogas sparging can reduce fouling at relatively lower gas flow rate than one at gas sparging only (Kim et al. 2014; Lee et al. 2006; Meier 2010; Rosenberger et al. 2011; Shim et al. 2015; Yang et al. 2006; Krause et al. 2010). Nevertheless, the biogas sparging still accounts for up to about 70% of total energy in AnMBR operation (Aslam et al. 2017b; Kurita et al. 2015; Martin et al. 2011; Seib et al. 2016; Verrecht et al. 2010).

Kim et al. (2011) developed new approach to control fouling with anaerobic fluidized bed membrane bioreactor (AFMBR). The AFMBR is to combine anaerobic fluidized bioreactor (AFBR) with submerged membrane filtration. Herein, granular activated carbon (GAC) particles are fluidized along membrane surface by recirculating a bulk suspension only through membrane reactor (Aslam et al. 2014; Shin et al. 2014; Wang et al. 2016; Ye et al. 2016). The GAC particles can provide high surface area for biofilm formation and scouring effect to reduce membrane fouling. Without biogas sparging, energy consumption required to fluidize GAC particles can be reduced significantly (less than 0.1 kWh/m^3) (Kim et al. 2011; Chaiprapat et al. 2016). Aslam et al. (2014) found that GAC fluidization reduced membrane fouling by adsorption of foulants and by the scouring action of GACs on membrane. However, after sorption capacity was diminished, then membrane scouring dominated (Aslam et al. 2017c; Lee et al. 2014; Remy et al. 2010; Wu et al. 2014).

While GAC fluidization is proven as an energy-efficient fouling mitigation way, the extent to which membrane fouling is understood can vary greatly depending upon the nature of the foulants and sizes of GAC particles. The objective of this study was to investigate membrane fouling with a laboratory-scale, fluidized membrane reactor to simulate AFMBR system with respect to the GAC sizes and feed solution which is effluent produced by AFBR. In spite of many advantages in fouling control, individual and collective behavior as membrane foulant and GAC fluidization is not well known through membrane scrubbing action. A better understanding of these effects will lead to improvements in the design and operation of the fluidized bed membrane bioreactor.

Materials and methods

Reactor configuration and operation

Figure 1 is a schematic of the experimental setup of a fluidized membrane reactor developed to observe fouling behavior under GAC fluidization. The fluidized membrane reactor was fabricated by using transparent acrylic column with 50 cm long by 2.5 cm diameter (effective volume 0.245 L). Two settlers were installed at top of the reactor to catch carryover the GAC particles as fluidized media. Each of the two joined settlers at the top of the reactor consisted of 10-cm-long × 7.5-cm-diameter tube (effective volume 0.442 L). Polyvinylidenefluoride (PVDF) hollow-fiber membranes with nominal pore size of 0.03 μm were submerged in the fluidized membrane reactor. Each fiber had 2.1 mm in outside diameter and 0.41 m long, resulting in an effective total membrane surface area of 0.0054 m^2. Prior to using the membranes, they were first soaked into 1000 ppm sodium hypochlorite solution for 12 h at room temperature followed by washing it with deionized water. The fibers were then soaked again into 2000 ppm citric acid solution for another 12 h to remove glycerol coating materials and maintain membrane wettability. The bulk suspension in the membrane reactor was recirculated by using a magnetic pump (Pan World magnetic pump, NH-100PX-Z, Korea) and a flow rate controller (Blue-White, F-450) to fluidize the GAC particles to cover the whole length of the hollow-fiber membranes. The membrane reactor was fed continuously by the effluent obtained from the pilot-scale, AFBR operated at domestic sewage plant. Filtrate of the effluent through 0.1-μm pore size of membrane was also tested as feed solution. The AFBR effluent was collected every week and stored in a refrigerator at 4 °C. All experimental works were performed at room temperature. General characteristics of AFBR effluent tested for feed solution in this study are shown in Table 1.

The feed solution was flowed into the membrane reactor by using a peristaltic pump (Masterflex, model no. 7520-57, USA) at a flow rate that was automatically controlled to maintain a constant water level. Open top sections of the hollow-fiber membranes submerged into the membrane reactor were connected to the peristaltic pump (Cole-Parmer, model no. 7553-85) at constant flux mode. The suction pressure required to maintain a given constant permeate flow rate was monitored with time by a vacuum pressure sensor (Cole-Parmer, model no. EW-68604-00) connected to the permeate line to monitor trans-membrane pressure (TMP) with filtration time as a fouling indicator.

Fluidized media and particle size fractionation

In this study, GAC particles (MRX-M, Calgon Carbon Coro., Pittsburgh, USA) were used as fluidized media to control
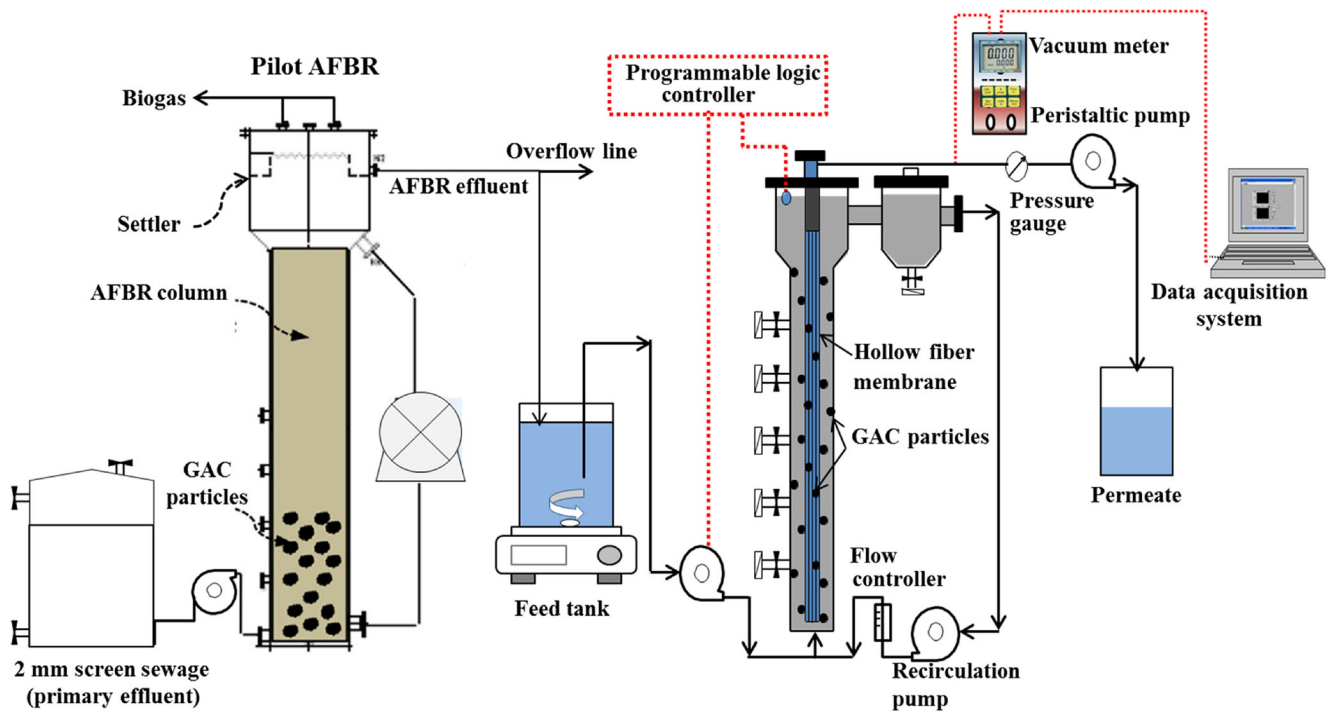
Fig. 1 Schematic diagram of fluidized membrane bioreactor treating effluent of pilot-scale anaerobic fluidized bed bioreactor for domestic wastewater treatment

membrane fouling. To exclude adsorption effect caused by GAC particles, their adsorption capacity was saturated fully by performing the adsorption column test using the same feed solution prior to fouling experiments. For this, the GAC particles were filled into the adsorption column reactor having 30-mm diameter and 470-mm height. The feed solution was passed through the adsorption column continuously, and the effluent from the column was analyzed by COD measurement with time until the effluent concentration equaled the influent concentration.

In order to investigate the effect of GAC size as fluidized media on membrane fouling, GAC particles were fractionated by sieves consisting of 6 × 10 and 35 × 80 meshes to classify 2000–3000 and 180–500 μm in GAC size, respectively. In this study, a GAC packing ratio was fixed at a 50% based upon total height of membrane reactor. The 50% of GAC packing ratio corresponded to 70, 67, and 73 g as GAC mass

Table 1 Mean concentrations of the AFBR effluent

Parameter	Unit	Mean concentration
Total organic carbon (TOC)	mg/L	63 ± 4.5
Total chemical oxygen demand (TCOD)	mg/L	174 ± 14
Soluble chemical oxygen demand (SCOD)	mg/L	88 ± 10
Total suspended solids (TSS)	mg/L	57 ± 7
Volatile suspended solids (VSS)	mg/L	48 ± 7
pH	–	6.92 ± 0.3

Values are given as ±standard deviation

for the mixed, 180–500 and 2000–3000 μm in distribution of GAC size, respectively. The upflow velocity required to fluidize each size range of GAC particle to cover the whole length of fibers was 0.031, 0.014, and 0.041 m/s, respectively.

Analysis of membrane fouling resistance in-series

In this study, the fouling resistance was estimated by Darcy's law described below.

$$J = \frac{\Delta P}{\mu R_t} \tag{1}$$

$$R_t = R_m + R_r + R_{ir} \tag{2}$$

where J is the membrane permeate flux (m³/m² s), ΔP is the TMP (Pa), μ is the permeate viscosity (Pa s), R_t is the total fouling resistance (m⁻¹), R_m is the bare membrane resistance (m⁻¹), R_r is the reversible fouling resistance (m⁻¹), and R_{ir} is the irreversible fouling resistance (m⁻¹). The TMP values collected over filtration time were used to calculate the total fouling resistance, R_t. The value of R_m was measured by filtering deionized water. After cleaning the membrane surface using a sponge to wipe off the fouling layer from membrane, the membrane permeability was then measured by deionized water to estimate $R_{ir} + R_m$ value. As a result, the R_{ir} could be given by the difference between R_m and $R_{ir} + R_m$ and the R_r was calculated by subtracting R_{ir} and R_m from R_t value subsequently.

Fouling rate was estimated by the difference between the initial and final fouling resistances divided by the duration of filtration as proposed (Fan and Zhou 2007).

$$F = \frac{R_{t2} - R_{t1}}{t_2 - t_1} \tag{3}$$

where R_{t1} and R_{t2} are the fouling resistance at filtration time of 20 min (t_1) and the time required to reach 0.3 bar of TMP (t_2), respectively. The initial fouling resistance was defined here as the fouling resistance after 20 min of filtration time to accommodate the effects of lag period required for the permeate pump to establish a stable vacuum through the system. The percentage of fouling contribution resulting from the fraction of each size range as fluidized media was then calculated as below:

$$F_{<0.1 \ \mu m}\% = \frac{F_{filtrate(0.1 \ \mu m)}}{F_{AFBReffluent}} \times 100 \tag{4}$$

$$F_{>0.1 \ \mu m}\% = \frac{F_{AFBReffluent} - F_{filtrate(0.1 \ \mu m)}}{F_{AFBReffluent}} \times 100 \tag{5}$$

where $F_{AFBR \ effluent}$ and $F_{filtrate(0.1 \ \mu m)}$ are the fouling rate caused by the AFBR effluent and by the effluent filtered through 0.1-μm membrane, respectively. Thus, $F_{>0.1 \ \mu m}$ represents the contribution of the particle sizes which are larger than 0.1 μm to membrane fouling.

Three-dimensional EEM fluorescence spectroscopy analysis

Three dimensional excitation-emission matrix (EEM) fluorescence spectra were measured to characterize the foulants extracted from the fouled membranes at the end of membrane operation. Fluorescence was measured in a 1-cm cuvette using a fluorescence spectrophotometer (F-4500, Hitachi, Japan) equipped with a 150-W xenon lamp at ambient temperatures (22 ± 1 °C). The fluorescence spectrum of Milli-Q water was subtracted from the spectra of each sample to eliminate the inner-filtering and metal binding effects. A fluorescence spectrum was obtained by collecting the wavelength of both excitations over a range of 230–450 nm and emission of 280–550 nm.

Liquid chromatography-organic carbon detection

Size exclusion liquid chromatography-organic carbon detection (LC-OCD; DOC-Labor Karlsruhe, Germany) analysis was performed to characterize the molecular weight of the soluble compounds and relative organic carbon in the AFBR effluent, the AFBR effluent filtered through 0.1-μm membrane, and the membrane permeate at the end of system operation. The LC-OCD analyzer contains a separating column in which compounds with large molecular weight elute before the smaller ones. The separated compounds are detected by

UV adsorption at 254 nm followed by organic carbon detection. The first peak of LC-OCD analysis at the organic carbon detector is a biopolymer peak representing proteins, polysaccharides, and organic colloids followed by humic substances, building blocks, organic acids, amphiphilic, and neutral substances. The UV chromatograms show similar distribution except for that polysaccharides are not detectable by UV light due to the absence of the double bonds which can adsorb the UV light (Siembida et al. 2010).

Results and discussion

GAC fluidization and membrane fouling

The TMP monitored with filtration time from the fluidized membrane reactor developed are compared for the AFBR effluent and its filtrate through 0.1-μm membrane. Results are shown in Fig. 2. Without GAC fluidization, the TMP value for the AFBR effluent as feed suspension approached to 0.3 bar within 1-day membrane operation. Prefiltration of the AFBR effluent through 0.1-μm membrane lowered fouling rate at the same permeate flux of 15 L/m² h. However, the time required to observe a 0.3 bar as TMP value could not be extended significantly (from 1 to 2 day of membrane operation), although the filtrate of AFBR effluent was applied as feed solution. This indicates that the contribution of the fine materials smaller than 0.1 μm to membrane fouling should not be overlooked.

The GAC fluidization along membrane surface was very effective to reduce membrane fouling with both unfiltered and filtered AFBR effluent as feed suspensions to the membrane. As also shown in Fig. 2, the time scale to observe the same TMP value of 0.3 bar was extended nearly by 11 and 3 times for the unfiltered and filtered feed solution, respectively. After 6.5 days of membrane operation, the TMP value for the raw (or unfiltered) feed solution jumped to 0.3 bar followed by gradual increase of it. Similar behavior in TMP increase was observed for the filtered sample by showing that TMP was jumped to 0.3 bar at 8.5-day operation. By using Eqs. 3–5, fouling contributions were estimated without and with GAC fluidization. As shown in Fig. 3, under the bulk recirculation only without GAC particles, it was found that about 20% in membrane fouling were contributed by the foulants smaller than 0.1 μm. However, this portion increased to about 80% under GAC fluidization, suggesting that the GAC scouring be less effective to remove small colloids away from the membrane.

At the end of membrane operation, fouling resistances were estimated by applying the resistance in-series models of Eqs. (1) and (2). Results are shown in Fig. 4. The reversible fouling resistance refers herein to the fouling resistance which can be removed by surface cleaning with a sponge and DI water as mentioned above. The irreversible fouling resistance is
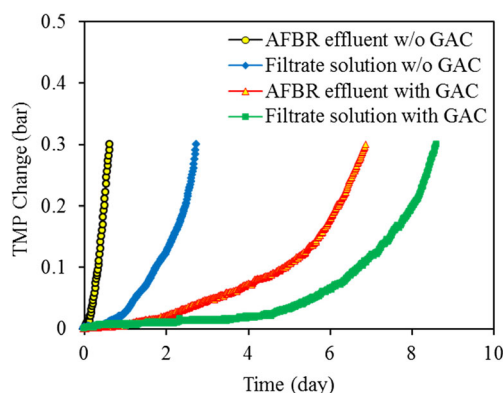
Fig. 2 TMP profiles for AFBR effluent and filtrate solution of 0.1-μm membrane (set-point permeate flux 15 L/m²h, spent mixed GAC packing ratio 50%, recirculation flow rate w/o GAC 3 L/min and with GAC 0.9 L/min)

Fig. 3 Contributions of foulant particle size on membrane fouling with and without GAC fluidization (set-point permeate flux 15 L/m²h, spent mixed GAC packing ratio 50%, recirculation flow rate w/o GAC 3 L/min and with GAC 0.9 L/min)

Fig. 4 Contributions of reversible and irreversible filtration resistances of the fouled membranes (set-point permeate flux 15 L/m²h, spent mixed GAC packing ratio 50%, recirculation flow rate w/o GAC 3 L/min and with GAC 0.9 L/min)

defined here as the fouling resistance which can be eliminated only through the membrane cleaning with NaOH solution. For the unfiltered feed solution, about 82% of the total fouling resistance was reversible without GAC fluidization. However, this reversible fouling resistance was greatly reduced by GAC fluidization. For the feed solution prefiltered through 0.1-μm membrane, about 86% of total fouling resistance were caused by irreversible fouling. These results indicate strongly that the GAC fluidization on membrane surface should reduce reversible fouling more effectively than irreversible fouling (Charfi et al. 2017). The rejection of the particulate and/or colloidal materials larger than the membrane pore size (0.03 μm) can induce build up of the cake layer on membrane. However, the GAC fluidization should delay cake formation due to its scouring action on membrane (Johir et al. 2013). Recently, Wu et al. (2017) reported that presence of GAC as scouring media reduced the cake resistance significantly but increased the irreversible fouling resistance. In another study, Kurita et al. (2014) applied polyethylene glycol granules as scouring media under gas sparging. They found that reversible fouling was entirely controlled by mechanical
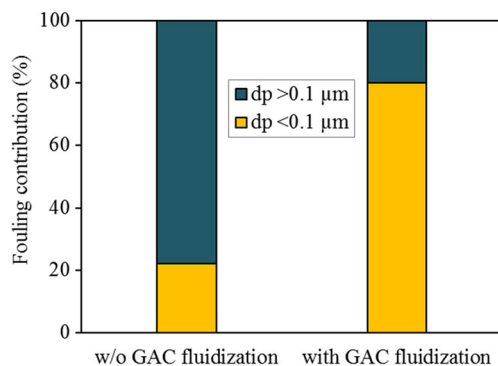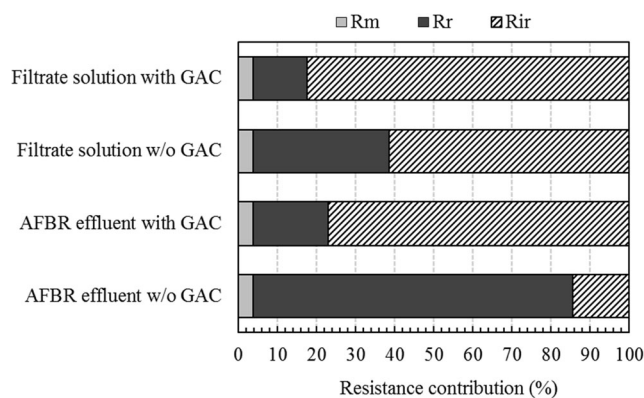
cleaning with scouring agent, but irreversible fouling was increased by cake layer elimination.

Characterizations of membrane fouling

In order to investigate dominant foulant materials on membrane surface after GAC fluidization, the fluorescent excitation-emission matrix (FEEM) analysis was performed using the foulant materials extracted from the used membrane. The foulants were extracted by soaking the fouled membranes into a NaOH solution for 1 day at the ambient temperature followed by ultra-sonication during 10 min. Results are demonstrated in Fig. 5. For the membranes taken from the membrane reactor without GAC fluidization, four distinct peaks were observed with both unfiltered and filtered feed solutions to membrane. In Fig. 5, first large peak detected at the excitation/emission (E_x/E_m) wavelength of 200–250/280–330 nm represents to the simple aromatic proteins such as tyrosine, which is indicated as A. The second and third peaks at the 250–340/280–380 nm (B) and 250–350/410–435 nm (C) are associated with the tryptophan proteins and natural dissolved organic matter described as the fluorescence of visible humic acid-like substances, respectively. The fourth peak located around the E_x/E_m of 240–260/390–470 nm (D) indicates fulvic-like substances (Chen et al. 2003). For the membranes exposed to the GAC particles, two additional peaks E and F were identified at 290/360 and 290/420 nm, corresponding to the peptides and tryptophan proteins and humic-like substances, respectively (Chen et al. 2003). The location of peak E (peptides and tryptophan-like) and peak F (humic-like) under GAC fluidization demonstrated a shift of fluorescence wavelength compared to that without GAC. This result indicates that large organic molecules should be broken into small fragments (Swietlik et al. 2004). The relative fluorescence intensities of the protein-like substances including tyrosine-like and tryptophan-like, humic and fulvic-like substances as foulant attributed to 57–70, 18–32, and 11–15%, respectively. The FEEM

Fig. 5 EEM fluorescence spectra of the extracted membrane foulants. **a** AFBR effluent w/o GAC fluidization. **b** AFBR effluent with GAC fluidization. **c** Filtrate solution w/o GAC fluidization. **d** Filtrate solution with GAC fluidization
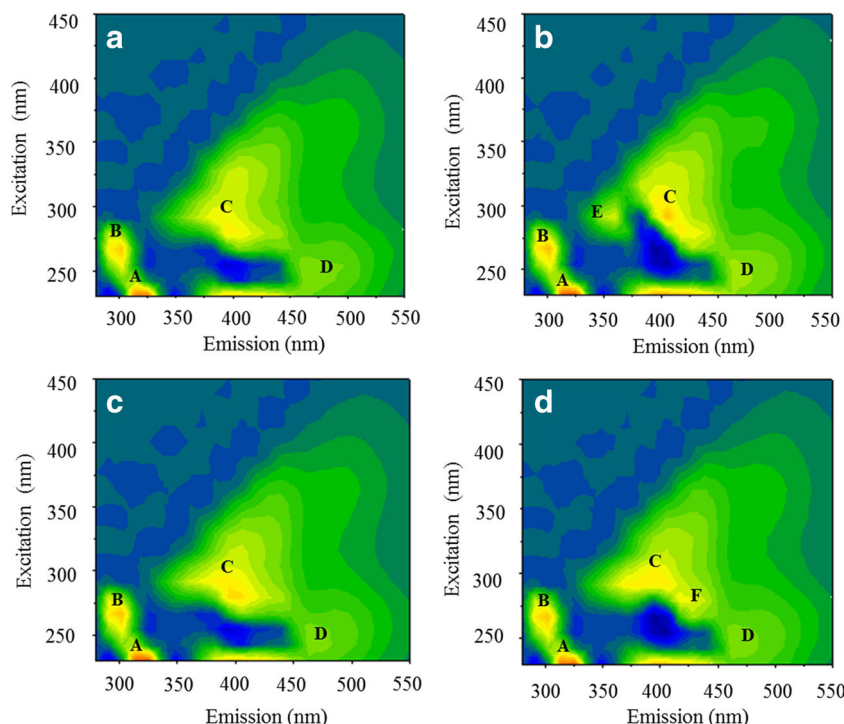
spectrum analysis suggests that the protein-like substances are most dominant foulant material for both unfiltered and filtered AFBR effluents as feed solution to membrane. As also observed in Fig. 5, a protein fraction is found to be more significant than the humic-like fraction for both feed suspensions.

The results of the LC-OCD analyses for the unfiltered, filtered feed solution, and the membrane permeate produced are shown in Fig. 6. For the unfiltered AFBR effluent and its filtrate through 0.1-μm membrane, large DOC peaks were found at the molecular weight (MW) bigger than 10,000 Da, supporting the biopolymers; a small UV peak corresponds to this. Since the UV peak is small, relative to DOC peaks, the eluted organic fraction comprises non-humic and low-aromatic structure such as protein and polysaccharides, which is evidenced also by FEEM results (Huber et al. 2011). Permeate through 0.03-μm membrane used for the fluidized bed membrane reactor had much smaller DOC peak at the same MW range than feed solutions. There is a much difference in the biopolymer DOC accumulation between the filtered sample as feed solution to the membrane and permeate through the 0.03-μm membrane pore used in this study. These results suggest that the accumulation of DOC that ranged from 0.03 to 0.1 μm in size should be biopolymers consisting of proteins and polysaccharides, but the FEEM analysis indicates that proteins be prevalent components in membrane foulants. Difference in the LC-OCD peaks representing to the humic-like substances and the low molecular organic acids was almost negligible. Explanation is that these small organic fractions can be passed through the membrane pores (0.03 μm) rather than being rejected by them. The proteins are generally

more hydrophobic and sticky in nature than other biofoulants (Li et al. 2012). The hydrophobic interactions between hydrophobic PVDF membrane used and biopolymers with strong stickiness properties should accelerate formation of membrane fouling (Lin et al. 2014). Nevertheless, the adhesion of biopolymers on membrane could also be explained by the intrinsic nature of this deposit. Hong et al. (2014) and Zhang et al. (2013) found that biopolymers in MBR should form a gel layer deposit on membrane and it could develop osmotic pressure during cake filtration. This gel layer can be formed with a thin layer resulted from the gelation of colloidal and dissolved matters/biofoulants (Chen et al. 2016), and the
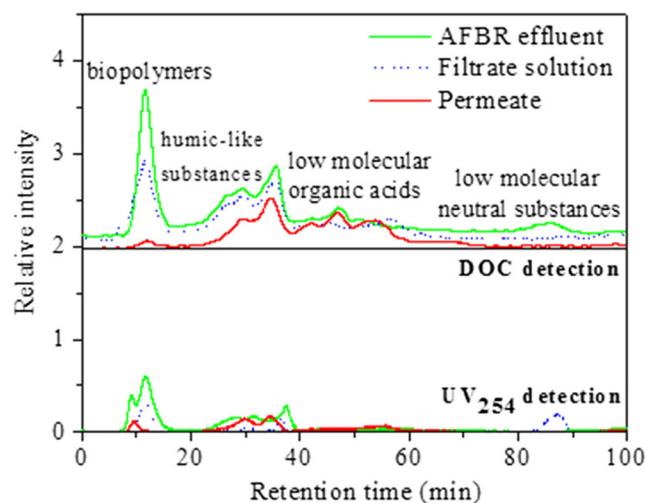

Fig. 6 LC-OCD analysis of AFBR effluent, filtrate of 0.1 μm, and fluidization-membrane reactor permeate

Fig. 7 TMP profiles with time using different GAC sizes and particle size fractions. **a** AFBR effluent as feed suspension. **b** Filtrate solution as feed suspension (set-point permeate flux 20 L/m²h, spent GAC packing ratio 50%, recirculation flow rate w/o GAC 3 L/min and with GAC size 2000–3000 μm 1.2 L/min and GAC size 180–500 μm 0.4 L/min)
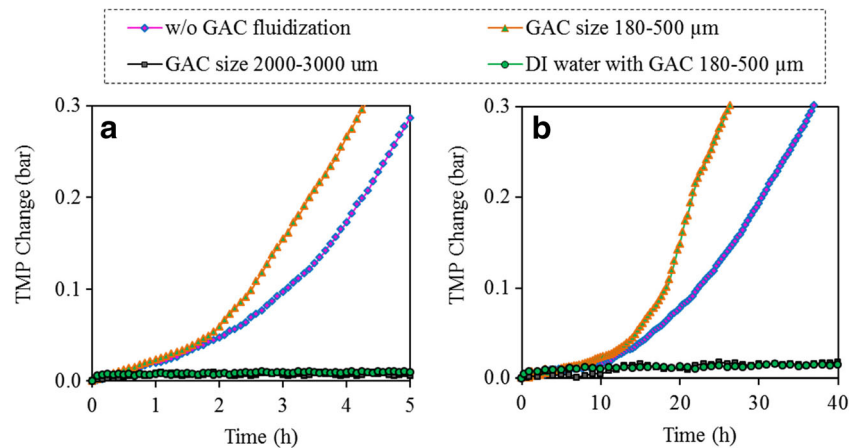
osmotic pressure through this layer provides main contributor to filtration resistance (Zhang et al. 2013). Although the gel layer can have high porosity and thin thickness, it can exhibit very high filtration resistance against hydraulic flows through membrane. The negatively charged functional groups carried by proteins which may be prevalent in the gel layer should be equivalent counter-ions present in the mixture of the layer. As a result, the chemical potential of permeate should be higher than that of water in the gel layer, providing osmotic pressure-induced resistance (Chen et al. 2016; Hong et al. 2014; Wang et al. 2008).

Effect of GAC size as fluidized media on membrane fouling

In Fig. 7a, biggest GAC sizes ranged from 2000 to 3000 μm tested results in greatest fouling control, showing no TMP jump during the whole filtration time. However, fluidization with smallest GAC particles tested in this study was not very

effective to reduce membrane fouling. As also shown in Fig. 7a, the TMP jump was started at 2 h of membrane filtration. Interestingly, fouling rate under the fluidization of these smallest GAC particles (180–500 μm) was even more severe than that observed under bulk recirculation only through the reactor without any GAC addition. This phenomenon was not observed in the same fluidized membrane reactor as the DI water was used as feed solution to membrane (Fig. S1). Formation of the fouling layer consisting of small carbon particles was clearly seen by SEM observations with fouled membranes after filtering sodium alginate (300 mg/L) and small GAC particles (180–500 μm) together (Fig. S2).

In this study, only mechanical cleaning action to control membrane fouling was considered because the GAC particles were adsorbed fully with test solution prior to their use. Large GAC particles in the range of 2000–3000 μm provided better scouring efficiency due to transferring higher momentum created in the vicinity of the membrane to the foulants (Charfi et al. 2017; Johir et al. 2013). Higher momentum can be
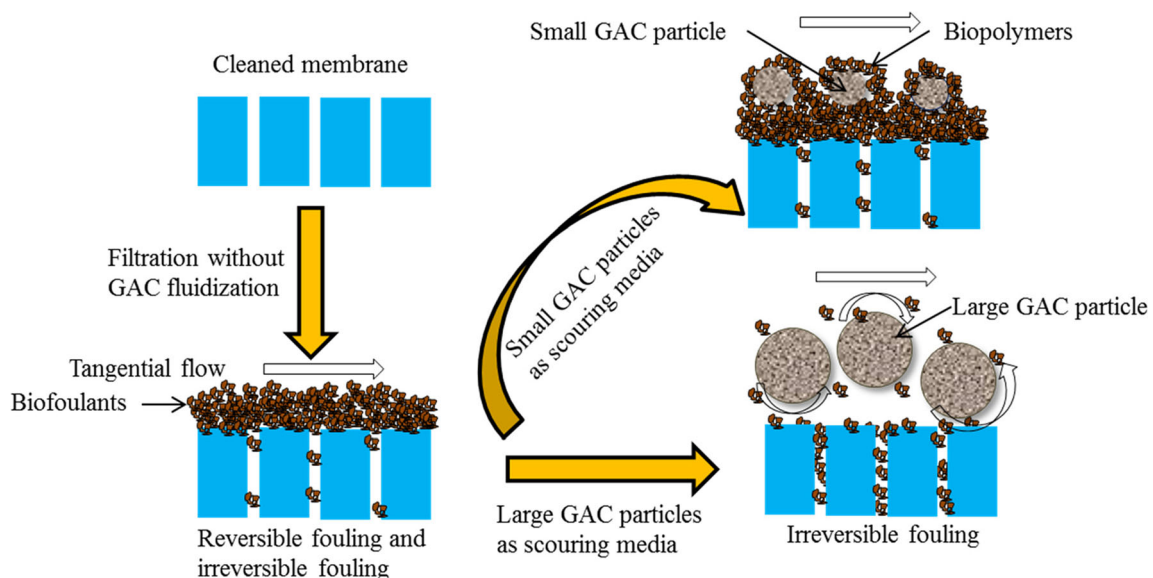

Fig. 8 Membrane fouling mechanism under fluidization of large (2000–3000 μm) and small (180–500 μm) GAC particles as scouring media

Fig. 9 TMP variation with time using different GAC sizes and particle size fractions at different set-point fluxes. **a** AFBR effluent as feed suspension. **b** Filtrate solution as feed suspension (spent GAC packing ratio 50%, recirculation flow rate w/o GAC 3 L/min and with GAC size 2000–3000 μm 1.2 L/min and mixed GAC size 0.9 L/min)
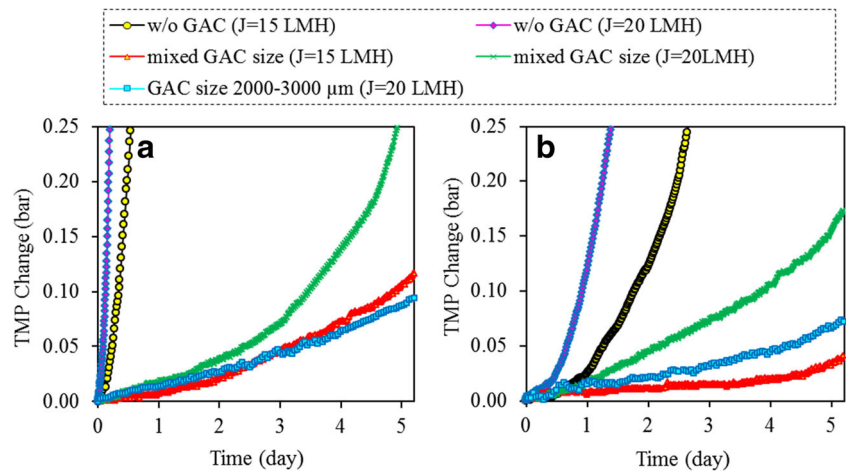

produced by larger fluidized media generating higher shear rate along membrane surface (Charfi et al. 2017). Smaller GAC particles (180–500 μm) tested in this study were less effective in fouling control than larger ones. In addition, deposit of the small GAC particles on membrane was severe providing surface fouling resistance. This deposit was facilitated by presence of organic materials of biopolymers on membrane (Fig. 8). Since floc size in the FMBR was larger than 1 μm (Fig. S3), a pore blockage due to the size may not contribute membrane fouling significantly. However, the presence of biopolymers should result in high filtration resistance due to facilitating attractive interactions causing high adhesion ability of small flocs/colloids to membrane (Shen et al. 2015).

Effect of set-point flux on membrane fouling is compared in Fig. 9. With the mixed GAC particles as fluidized media, higher set-point flux resulted in higher fouling rate as expected. However, the largest GAC with 2000–3000 μm in size range reduces membrane fouling effectively at higher set-point flux than that observed under the fluidization of the mixed GAC particles as fluidized media (15 vs. 20 L/m² h). Same results were also observed for both feed solutions of AFBR effluent and its filtrate through 0.1-μm membrane.

Fig. 10 SEM images of the membrane surface and cross section **a**, **b** for virgin membrane and **c**, **d** for used FMBR membrane after fluidization with large GAC size 2000–3000 μm (after chemical cleaning)
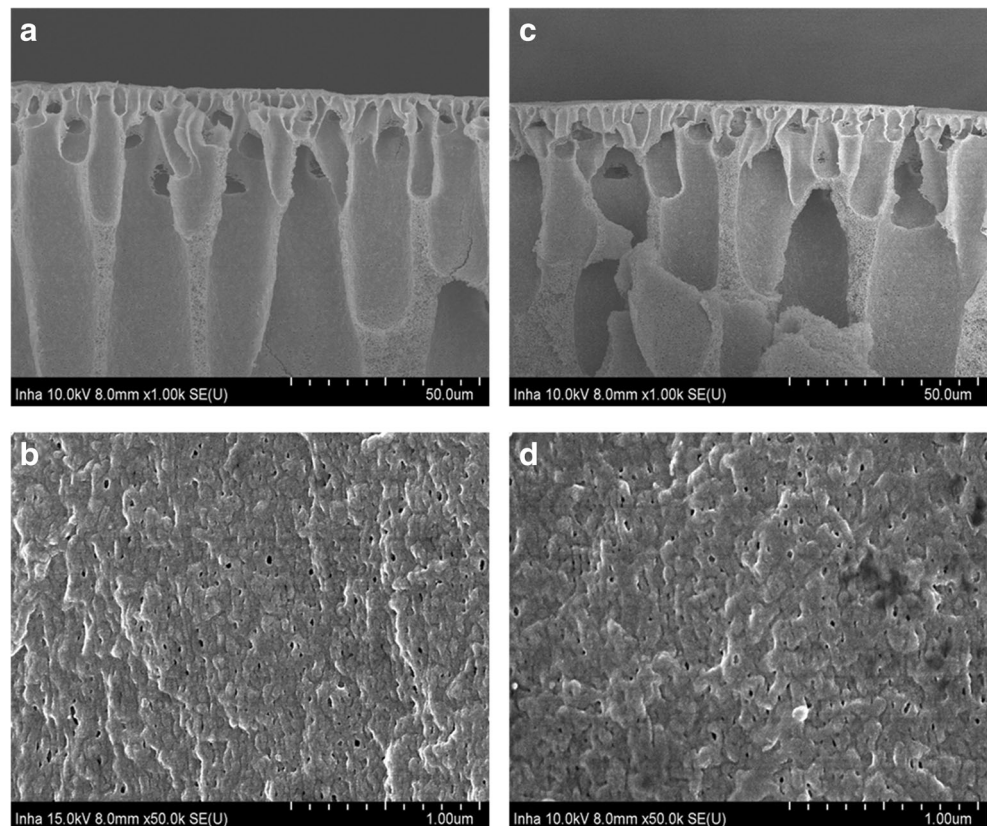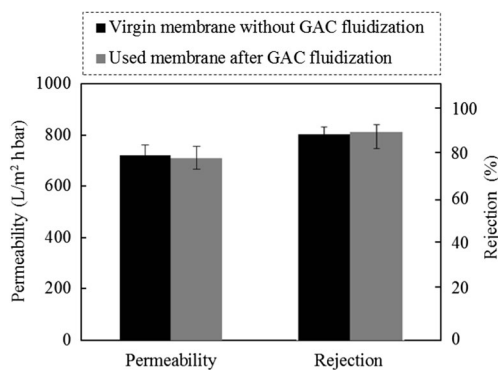
Fig. 11 Membrane permeability and sodium alginate rejection for virgin membrane and used FMBR membrane after fluidization with large GAC size 2000–3000 μm (after chemical cleaning and filtration time 30 min)

GAC fluidization and membrane integrity

There is a potential risk that the direct contact of fluidized GAC with especially large particle sizes with membrane surface removes cake layer and causes membrane damage due to their scouring actions. SEM observations through membrane surface and cross section of the virgin membrane and used membrane after chemical cleaning operated under the fluidization of large GAC size (2–3 mm) were compared (Fig. 10). The cross-sectional SEM image of the used membrane revealed that appearance of membrane skin layer was close to that of the virgin membrane even after GAC abrasion. Morphological observations of membrane surface and pore structure are close to the virgin membrane. Figure 11 shows the comparison of clean water permeability and rejection with sodium alginate between used membrane after recovery cleaning and virgin membrane. Average permeability with used membrane was 720 ± 45 L/m^2 h bar, which is close to the range employed by the virgin membrane of 700–800 L/m^2 h bar provided by the membrane manufacturer. In addition, there is no difference in membrane rejection of sodium alginate between the used and virgin membrane. In spite of excellent tool with GAC fluidization in fouling control, further works are still needed to know the influence of media shape and their usage time on membrane integrity (Di Natale and Nigro 2016).

For the filtrate solution, however, the scouring efficiency to reduce membrane fouling under the fluidization of the 2000–3000-μm-sized GAC particles was relatively limited. This phenomena became more apparent when the permeate flux increased to 20 L/m^2 h.

As permeate flux increases, the foulants smaller than 0.1 μm contributes membrane fouling considerably. This indicates that the presence of larger particles existing in the bulk solution on membrane can provide synergistic effect on fouling mitigation under GAC fluidization. Kurita et al. (2014) observed beneficial effect of large particulate materials present in bulk solution to the membrane on reducing irreversible fouling resistance under the fluidization of polyethylene glycol media. Geng et al. (2009) also reported that the presence of relatively large particulate in the bulk solution acted like moving barriers, and this can intercept fine colloids toward membrane.

Concern is that GAC fluidization may release micro- and nano-scaled carbon particles due to collisions between the particles. Change into smaller carbon particles as fluidized media may reduce scouring efficiency due to lowering momentum induced along membrane surface. In order to know whether GAC fluidization changes carbon particle sizes, they were fluidized at 0.9 L/min of recirculation flow rate for 10 days along the membrane surface using deionized water. At the end of fluidization, the GAC particles were taken from the reactor for measuring their particle size distribution. For this test, deionized water was used to improve more direct contact between the GAC particles. Deposit of the foulants on GAC particles may influence their net abrasive actions (Wu et al. 2016). There was no change in the particle size distribution of the GACs before and after experiments. Figure S4 indicates that the bulk recirculation through the laboratory-scaled, fluidized membrane reactor does not release any small carbon particles during the operational period in this study.

Conclusions

Mechanical cleaning efficiency by GAC fluidization is dependent strongly upon GAC size and the particle size as target foulant into fluidized bed membrane reactor. Fouling control was more pronounced with bigger GAC particles as fluidized media, but the effectiveness was less pronounced smaller foulants than 0.1 μm in size due to irreversible fouling resistance. Biopolymers such as proteins were rejected by membranes, causing significant membrane fouling in comparison to other organic fractions such as humic-like substances and low-molecular weight organic acids. The use of smaller GAC particles as fluidized media provided somewhat limited effect on fouling reduction. In addition, severe deposit of small GAC particles on membrane was driven by biopolymers rejected by the membranes, facilitating fouling rate.

References

Ahmad R, Ahmad Z, Khan AU, Mastoi NR, Aslam M, Kim J (2016) Photocatalytic systems as an advanced environmental remediation: recent developments, limitations and new avenues for applications. J Environ Chem Eng 4:4143–4164

Alresheedi MT, Basu OD (2014) Support media impacts on humic acid, cellulose, and kaolin clay in reducing fouling in a submerged hollow fiber membrane system. J Membr Sci 450:282–290

Aslam M, McCarty PL, Bae J, Kim J (2014) The effect of fluidized media characteristics on membrane fouling and energy consumption in anaerobic fluidized membrane bioreactors. Sep Purif Technol 132: 10–15

Aslam M, Lee P-H, Kim J (2015) Analysis of membrane fouling with porous membrane filters by microbial suspensions for autotrophic nitrogen transformations. Sep Purif Technol 146:284–293

Aslam M, Charfi A, Lesage G, Heran M, Kim J (2017a) Membrane bioreactors for wastewater treatment: a review of mechanical cleaning by scouring agents to control membrane fouling. Chem Eng J 307:897–913

Aslam M, Charfi A, Kim J (2017b) Membrane scouring to control fouling under fluidization of non-adsorbing media for wastewater treatment. Environ Sci Pollut Res. doi:10.1007/s11356-017-8527-2

Aslam M, McCarty PL, Shin C, Bae J, Kim J (2017c) Low energy single-staged anaerobic fluidized bed ceramic membrane bioreactor (AFCMBR) for wastewater treatment. Bioresour Technol 240:33–41

Aslan M, Saatçi Y, Hanay Ö, Hasar H (2014) Effect of biogas sparging with different membrane modules on membrane fouling in anaerobic submerged membrane bioreactor (AnSMBR). Environ Sci Pollut Res 21:3285–3293

Chaiprapat S, Thongsai A, Charnnok B, Khongnakorn W, Bae J (2016) Influences of liquid, solid, and gas media circulation in anaerobic membrane bioreactor (AnMBR) as a post treatment alternative of aerobic system in seafood industry. J Membr Sci 509:116–124

Charfi A, Amar NB, Harmand J (2012) Analysis of fouling mechanisms in anaerobic membrane bioreactors. Water Res 46:2637–2650

Charfi A, Aslam M, Lesage G, Heran M, Kim J (2017) Macroscopic approach to develop fouling model under GAC fluidization in anaerobic fluidized bed membrane bioreactor. J Ind Eng Chem 49: 219–229

Chen W, Westerhoff P, Leenheer JA, Booksh K (2003) Fluorescence excitation-emission matrix regional integration to quantify spectra for dissolved organic matter. Environ Sci Technol 37:5701–5710

Chen J-R, Zhang M, Li F, Qian L, Lin H-J, Yang L, Wu X, Zhou X, He Y-M, Liao B-Q (2016) Membrane fouling in a membrane bioreactor: high filtration resistance of gel layer and its underlying mechanisms. Water Res 102:82–89

Di Natale F, Nigro R (2016) An experimental procedure to estimate tube erosion rates in bubbling fluidised beds. Powder Technol 287:96–107

Díaz O, Vera L, González E, García E, Rodríguez-Sevilla J (2016) Effect of sludge characteristics on membrane fouling during start-up of a tertiary submerged membrane bioreactor. Environ Sci Pollut Res 23: 8951–8962

Fan F, Zhou H (2007) Interrelated effects of aeration and mixed liquor fractions on membrane fouling for submerged membrane bioreactor processes in wastewater treatment. Environ Sci Technol 41:2523–2528

Geng Z, Hall ER, Bérubé PR (2009) Roles of various mixed liquor constituents in membrane filtration of activated sludge. Desalin Water Treat 1:139–149

Ghauri M, Bokari A, Aslam M, Tufail M (2011) Biogas reactor design for dry process and generation of electricity on sustainable basis. Int J Chem Environ Eng 2:414–417

Hong H, Zhang M, He Y, Chen J, Lin H (2014) Fouling mechanisms of gel layer in a submerged membrane bioreactor. Bioresour Technol 166:295–302

Hu J, Ren H, Xu K, Geng J, Ding L, Yan X, Li K (2012) Effect of carriers on sludge characteristics and mitigation of membrane fouling in attached-growth membrane bioreactor. Bioresour Technol 122:35–41

Huang X, Wei C-H, Yu K-C (2008) Mechanism of membrane fouling control by suspended carriers in a submerged membrane bioreactor. J Membr Sci 309:7–16

Huber SA, Balz A, Abert M, Pronk W (2011) Characterisation of aquatic humic and non-humic matter with size-exclusion chromatography-organic carbon detection-organic nitrogen detection (LC-OCD-OND). Water Res 45:879–885

Jin L, Ong SL, Ng HY (2013) Fouling control mechanism by suspended biofilm carriers addition in submerged ceramic membrane bioreactors. J Membr Sci 427:250–258

Johir M, Shanmuganathan S, Vigneswaran S, Kandasamy J (2013) Performance of submerged membrane bioreactor (SMBR) with and without the addition of the different particle sizes of GAC as suspended medium. Bioresour Technol 141:13–18

Kim J, Kim K, Ye H, Lee E, Shin C, McCarty PL, Bae J (2011) Anaerobic fluidized bed membrane bioreactor for wastewater treatment. Environ Sci Technol 45:576–581

Kim J, Shin J, Kim H, Lee J-Y, Yoon M-H, Won S, Lee B-C, Song KG (2014) Membrane fouling control using a rotary disk in a submerged anaerobic membrane sponge bioreactor. Bioresour Technol 172: 321–327

Krause S, Zimmermann B, Meyer-Blumenroth U, Lamparter W, Siembida B, Cornel P (2010) Enhanced membrane bioreactor process without chemical cleaning. Water Sci Technol 61:2575–2580

Krzeminski P, van der Graaf JHJM, van Lier JB (2012) Specific energy consumption of membrane bioreactor (MBR) for sewage treatment. Water Sci Technol 65:380–392

Kurita T, Kimura K, Watanabe Y (2014) The influence of granular materials on the operation and membrane fouling characteristics of submerged MBRs. J Membr Sci 469:292–299

Kurita T, Kimura K, Watanabe Y (2015) Energy saving in the operation of submerged MBRs by the insertion of baffles and the introduction of granular materials. Sep Purif Technol 141:207–213

Le-Clech P, Chen V, Fane TAG (2006) Fouling in membrane bioreactors used in wastewater treatment. J Membr Sci 284:17–53

Lee W-N, Kang I-J, Lee C-H (2006) Factors affecting filtration characteristics in membrane-coupled moving bed biofilm reactor. Water Res 40:1827–1835

Lee R, McCarty PL, Bae J, Kim J (2014) Anaerobic fluidized membrane bioreactor polishing of baffled reactor effluent during treatment of dilute wastewater. J Chem Technol Biotechnol 90:391–397

Li J, Yang F, Liu Y, Song H, Li D, Cheng F (2012) Microbial community and biomass characteristics associated severe membrane fouling during start-up of a hybrid anoxic–oxic membrane bioreactor. Bioresour Technol 103:43–47

Liao B-Q, Kraemer JT, Bagley DM (2006) Anaerobic membrane bioreactors: applications and research directions. Crit Rev Environ Sci Technol 36:489–530

Lin H, Gao W, Meng F, Liao B-Q, Leung K-T, Zhao L, Chen J, Hong H (2012) Membrane bioreactors for industrial wastewater treatment: a critical review. Crit Rev Environ Sci Technol 42:677–740

Lin H, Zhang M, Wang F, Meng F, Liao B-Q, Hong H, Chen J, Gao W (2014) A critical review of extracellular polymeric substances (EPSs) in membrane bioreactors: characteristics, roles in membrane fouling and control strategies. J Membr Sci 460:110–125

Martin I, Pidou M, Soares A, Judd S, Jefferson B (2011) Modelling the energy demands of aerobic and anaerobic membrane bioreactors for wastewater treatment. Environ Technol 32:921–932

Meier J (2010) Mechanical influence of PAC particles on membrane processes. J Membr Sci 360:404–409

Meng F, Chae S-R, Drews A, Kraume M, Shin H-S, Yang F (2009) Recent advances in membrane bioreactors (MBRs): membrane fouling and membrane material. Water Res 43:1489–1512

Meng F, Zhang S, Oh Y, Zhou Z, Shin H-S, Chae S-R (2017) Fouling in membrane bioreactors: an updated review. Water Res 114:151–180

Ng CA, Sun D, Bashir MJ, Wai SH, Wong LY, Nisar H, Wu B, Fane AG (2013) Optimization of membrane bioreactors by the addition of powdered activated carbon. Bioresour Technol 138:38–47

Nguyen T-T, Bui X-T, Nguyen D-D, Nguyen P-D, Ngo H-H, Guo W (2016) Performance and membrane fouling of two types of laboratory-scale submerged membrane bioreactors for hospital wastewater treatment at low flux condition. Sep Purif Technol 165:123–129

Ozgun H, Dereli RK, Ersahin ME, Kinaci C, Spanjers H, van Lier JB (2013) A review of anaerobic membrane bioreactors for municipal wastewater treatmet: integration options, limitations and expectations. Sep Purif Technol 118:89–104

Pradhan M, Vigneswaran S, Kandasamy J, Ben Aim R (2012) Combined effect of air and mechanical scouring of membranes for fouling reduction in submerged membrane reactor. Desalination 288:58–65

Remy M, Potier V, Temmink H, Rulkens W (2010) Why low powdered activated carbon addition reduces membrane fouling in MBRs. Water Res 44:861–867

Rosenberger S, Helmus FP, Krause S, Bareth A, Meyer-Blumenroth U (2011) Principles of an enhanced MBR-process with mechanical cleaning. Water Sci Technol 64:1951–1958

Seib MD, Berg KJ, Zitomer DH (2016) Low energy anaerobic membrane bioreactor for municipal wastewater treatment. J Membr Sci 514:450–457

Shen L-G, Lei Q, Chen J-R, Hong H-C, He Y-M, Lin H-J (2015) Membrane fouling in a submerged membrane bioreactor: impact of floc size. Chem Eng J 269:328–334

Shim SN, Kim S-R, Jo SJ, Yeon K-M, Lee C-H (2015) Evaluation of mechanical membrane cleaning with moving beads in MBR using Box–Behnken response surface methodology. Desalin Water Treat 56:2797–2806

Shin C, McCarty PL, Kim J, Bae J (2014) Pilot-scale temperate-climate treatment of domestic wastewater with a staged anaerobic fluidized membrane bioreactor (SAF-MBR). Bioresour Technol 159:95–103

Siembida B, Cornel P, Krause S, Zimmermann B (2010) Effect of mechanical cleaning with granular material on the permeability of submerged membranes in the MBR process. Water Res 44:4037–4046

Skouteris G, Hermosilla D, Pez PLO, Negro C, Blanco AN (2012) Anaerobic membrane bioreactors for wastewater treatment: a review. Chem Eng J 198:138–148

Smith AL, Stadler LB, Love NG, Skerlos SJ, Raskin L (2012) Perspectives on anaerobic membrane bioreactor treatment of domestic wastewater: a critical review. Bioresour Technol 122:149–159

Stuckey DC (2012) Recent developments in anaerobic membrane reactors. Bioresour Technol 122:137–148

Swietlik J, Dabrowska A, Raczyk-Stanisławiak U, Nawrocki J (2004) Reactivity of natural organic matter fractions with chlorine dioxide and ozone. Water Res 38:547–558

Verrecht B, Maere T, Nopens I, Brepols C, Judd S (2010) The cost of a large-scale hollow fibre MBR. Water Res 44:5274–5283

Wang Z, Wu Z, Yin X, Tian L (2008) Membrane fouling in a submerged membrane bioreactor (MBR) under sub-critical flux operation: membrane foulant and gel layer charcterization. J Membr Sci 325:238–244

Wang Z, Ma J, Tang CY, Kimura K, Wang Q, Han X (2014) Membrane cleaning in membrane bioreactors: a review. J Membr Sci 468:276–307

Wang J, Zamani F, Cahyadi A, Toh JY, Yang S, Wu B, Liu Y, Fane AG, Chew JW (2016) Correlating the hydrodynamics of fluidized granular activated carbon (GAC) with membrane-fouling mitigation. J Membr Sci 510:38–49

Wu B, Wong PCY, Fane AG (2014) The potential roles of granular activated carbon in anaerobic fluidized membrane bioreactors: effect on membrane fouling and membrane integrity. Desalin Water Treat 53:1450–1459

Wu B, Wang Y, Lim W, Chew JW, Fane AG, Liu Y (2016) Enhanced performance of submerged hollow fibre microfiltration by fluidized granular activated carbon. J Membr Sci 499:47–55

Wu B, Zamani F, Lim W, Liao D, Wang Y, Liu Y, Chew JW, Fane AG (2017) Effect of mechanical scouring by granular activated carbon (GAC) on membrane fouling mitigation. Desalination 403:80–87

Yang Q, Chen J, Zhang F (2006) Membrane fouling control in a submerged membrane bioreactor with porous, flexible suspended carriers. Desalination 189:292–302

Ye Y, LaBarge N, Kashima H, Kim K-Y, Hong P-Y, Saikaly PE, Logan BE (2016) An aerated and fluidized bed membrane bioreactor for effective wastewater treatment with low membrane fouling. Environ Sci: Water Res Technol 2:994–1003

Yu D, Chen Y, Wei Y, Wang J, Wang Y, Li K (2017) Fouling analysis of membrane bioreactor treating antibiotic production wastewater at different hydraulic retention times. Environ Sci Pollut Res 24:9026–9035

Zhang M, Peng W, Chen J, He Y, Ding L, Wang A, Lin H, Hong H, Zhang Y, Yu H (2013) A new insight into membrane fouling mechanism in a submerged membrane bioreactor: osmotic pressure during cake layer filtration. Water Res 47:2777–2786